(BL8B2) Photoelectron spectra of metallofullerene, $Sc@C_{82}$

Shojun Hino[a,b], Kazunori Umishita[a,b] Kentaro Iwasaki[a], Takayuki Miyamae[b,c],
Masayasu Inakuma[d] and Hisanori Shinohara[d]

[a] *Faculty of Engineering, Chiba University, Inage-ku, Chiba 263-8522 Japan*

[b] *Graduate School of Science and Technology, Chiba University, Inage-ku, Chiba 263-8522 Japan*

[c] *Institute for Molecular Science, Myoudaiji, Okazaki, Japan 444-8585*

[d] *Faculty of Science, Nagoya University, Chikusa-ku, Nagoya 464-8602 Japan*

Metallofullerenes have attracted a lot of attentions such as their structures including the position of the metal atom(s), their electronic structures as well as the amounts of transferred electrons from the metal atom(s) to the cage, their reactivity and so on. Photoelectron spectroscopy is a powerful tool to clarify their electronic structures. In this article, our recent results of the photoelectron spectroscopy on metallofullerene, $Sc@C_{82}$ are presented and its electronic structures are discussed.

Figure 1 shows the incident photon energy dependence of the UPS of the $Sc@C_{82}$ sublimed film. A clear intensity variation is observed in the UPS of $Sc@C_{82}$ as reported on other fullerenes [1-5]. Particularly, structures A and B vary their intensity drastically with the incident photon energy. Their intensities in the $h\nu$ = 20 and 40 eV spectra are nearly equal, but in other spectra structure B is about one and half times more intense than A. A similar energy dependence is observed in the UPS of C_{82} [2] and $La@C_{82}$ [1]. A close inspection reveals that structure N also changes its intensity as other structures.

Figure 2 shows the UPS of $Sc@C_{82}$ and $La@C_{82}$ with that of empty fullerene C_{82} obtained with 40 eV photon that gives the spectra having clear peak structures. These spectra look analogous; each of structures A – E have almost the same intensity and show one-to-one correspondence as indicated by chain lines. While significant shifts are observed in the energy positions of structures A and E, structures B – D have nearly identical binding energies. The shift of structure E may be due to a difference in the geometry of these fullerenes; C_2 for C_{82} and C_{2v} for these metallofullerenes. The troughs between the structures, such as those at about 4 and 6 eV, in the spectra of metallofullerenes are shallower than their counterparts in C_{82}. This may also be due to a difference in the geometry or to a change in the electronic structure caused by encapsulation of the metal atom to the cage.

The difference spectra obtained by subtraction of the 20 eV spectrum of empty C82 from those of metallofullerenes are shown in Fig. 3. There is a widely spread band between the E_F and 2.2 eV (upper valence band region) in both spectra. There is no significant structure

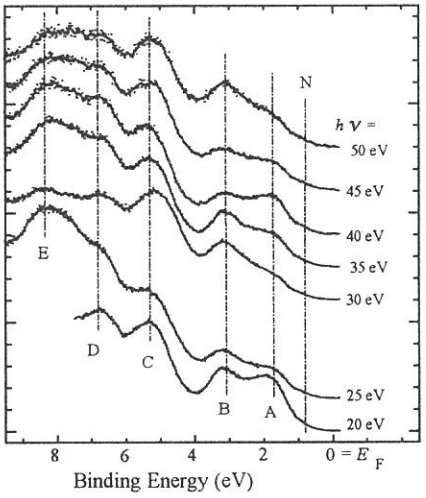

Fig. 1 The UPS of $Sc@C_{82}$

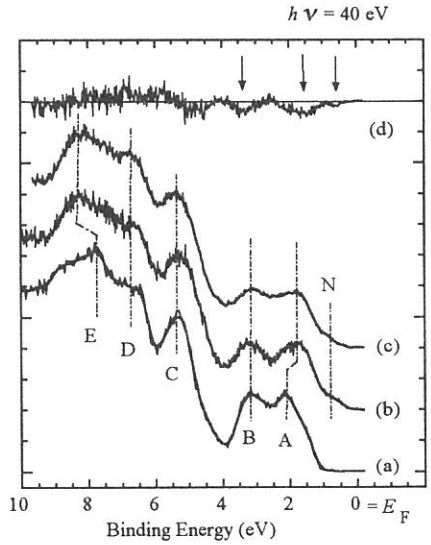

Fig. 2 The UPS of empty C_{82} (a), $La@C_{82}$ (b) and $Sc@C_{82}$ (c) with difference spectrum (d) between (b) and (c).

between 2.2 and 3.5 eV. Another evident band appears from 3.5 eV and deeper. This wide band is partly contributed from structure N that is not observed in the spectra of C_{82} and partly from the intensity difference in structure A. This band is considered to be due to the electrons transferred from the metal atom, since electrons from the Sc and La are expected to fill the LUMO of C_{82} and upwards. The band located beyond 3.5 eV is probably due to the intrinsic difference in the electronic structures of metallofullerenes and empty fullerene.

The peak area of the wide band in the Sc@C_{82} – C_{82} difference spectrum is smaller than that in La@C_{82} – C_{82}, and their ratio is about 2 : 3. This suggests that the amount of transferred electrons in Sc@C_{82} is about two thirds of that in La@C_{82}. Namely, two and three electrons are transferred from Sc and La to C_{82}, respectively. This is noteworthy, since both scandium and lanthanum are trivalent elements and their + 3 oxidation state is expected as the most stable one.

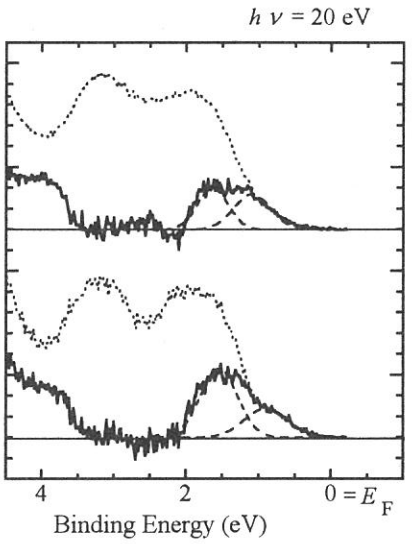

Fig. 3 Difference spectra Sc@C_{82} – C_{82} (upper) and La@C_{82} – C_{82} (lower).

References

1. S. Hino *et al.*, Phys. Rev. Letters 71, (1993) 4261.
2. S. Hino *et al.*, Phys. Rev. B 48, (1993) 8418.
3. J. H. Weaver *et al.*, Phys. Rev. Letters 66, (1991) 1741.
4. S. Hino *et al.*, Chem. Phys. Letters 190, (1992) 169.
5. S. Hino *et al.*, Phys. Rev. B 53, (1996) 7496.

(BL8B2)

Origin of the photoemission intensity oscillation of C_{60}

Shinji Hasegawa, Takayuki Miyamae, Kyuya Yakushi, Hiroo Inokuchi, Kazuhiko Seki[a], Nobuo Ueno[b]
Institute for Molecular Science, Myodaiji, Okazaki 444-8585, Japan
[a] *Department of Chemistry, Faculty of Science, Nagoya University, Nagoya 464-8602, Japan*
[b] *Department of Materials Science, Faculty of Engineering, Chiba University, Inage-ku Chiba 263-8522*

The photoemission intensities of the highest occupied molecular orbital (HOMO) and the next-HOMO (NHOMO) states for thin films, single crystals and gas phase of C_{60} exhibit remarkable oscillations with the incident photon energy in the range of $h\nu$= 10 – 120eV [1], and much attention has been paid to the phenomenon. From theoretical points of view, Xu *et al.* first reported two simple models to explain these oscillations [2]. They approximated the initial and final state wave functions with the radial and angular parts in the spherically symmetric potential of C_{60}, and calculated the energy positions of the cross section minima by using one of the allowed states ($l_f = l_i - 1$). They concluded that the oscillations originate from a specific ability of C_{60} to form a spherical standing wave of the final state by the interference inside the molecule. As mentioned by themselves, however, more detailed and quantitative studies are required to confirm the origin of the oscillations.

We measured the angle-resolved ultraviolet photoelectron spectra (ARUPS) of C_{60} thin films in the photon energy range of $h\nu$= 18 – 110 eV, and calculated the $h\nu$ dependences of the differential photoionization cross sections by changing the degree of approximation for the final and initial states [3]. First we carried out the numerical calculations by the single-scattering approximation for the final state with the *ab-initio* molecular orbital (MO) calculation for the initial state, where the angular parameters for the incident light and the photoelectron momentum were identical with the experimental conditions. It is noted that such quantitative calculations considering the scattering effects, to our knowledge, have not been reported yet for C_{60}. Next we simplified only the final state, and calculated the photoionization cross sections by using the plane-wave final state. In Fig.1, the measured and calculated $h\nu$ dependences of the intensity ratio, HOMO/NHOMO, are shown. Both calculated curves are based on the interference of photoelectron waves, since they are made up of a sum of the individual photoelectron wave from each atomic site with its phase difference. Therefore, the agreement between the calculated and measured results in Fig.1 suggests that the oscillation originates from the interference of photoelectron waves emanating from each atom constituting the C_{60} molecule, *i.e.*, the multi-centered photoemission from the MO state. Further, it should be noted that the calculated result by the simplest plane-wave approximation for the final state exhibits the similar oscillation as the measured one. This points out that the oscillation itself is independent of the accuracy of the final state. It should be ruled by a specific character of the initial state due to the molecular geometry of C_{60}.

In order to clarify this point, we approximated the MO initial state by a spherical-shell like state, and derived a simple formula for the differential photoionization cross section as [3],

$$d\sigma_n^{pw}(\mathbf{k}_n)/d\hat{\mathbf{r}} \quad \propto \quad \frac{h\nu}{k_n}\{\int \cos(k_n r + \alpha_{l_i} - \frac{l_i}{2}\pi)\Theta(r)r^2 dr\}^2. \tag{1}$$

To evaluate the eq.(1) by a simple analytical calculation, we approximate the radial part of initial state $\Theta(r)$ by step functions as,

$$\Theta(r) = \begin{cases} -\xi & \mathrm{R}_s - \Delta \le r \le \mathrm{R}_s \\ \xi & \mathrm{R}_s \le r \le \mathrm{R}_s + \Delta. \end{cases} \tag{2}$$

R_s and Δ stand for the radius of the node in the spherical shell and the half width of the shell, respectively. Consequently, the integral in eq.(1) is easily solved and the differential photoionization cross section at a given photon energy $h\nu$ can be calculated. In Fig.2, the calculated $h\nu$ dependences of the photoionization

cross section for the HOMO and NHOMO states are plotted with E_k. The solid curves are the results by the spherical-shell like initial state and the plane-wave final state, where we used the parameters R_s= 3.26Å, Δ= 0.5Å. The values are reasonable, since R_s= 3.26Å is close to 3.54Å of the radius of C_{60}, and Δ= 0.5Å was referred to the average half thickness of the deep potential shell for carbon solids. The broken curves are the same results as shown in Fig.1 calculated by the STO-5G MO initial state and the single-scattering final state. Note that the broken curves represent the intensity oscillations for the HOMO and NHOMO states before deriving their ratio in Fig.1. In spite of the present rough approximations for the initial and final states, the simple calculations with eq.s(1) and (2) give the equal oscillations as obtained by the more sophisticated calculations in regard to the energy positions of maxima and minima for both states (Eq.(2) is too rough to discuss the exact photoemission intensities. This may be the reason for the intensity difference between the solid and broken curves.). It means that the simplest model contains an essential point for the oscillations, that is, the spherical-shell like initial state due to the specific structure of C_{60} dominates the oscillations.

In addition, the radius of the spherical shell is also important to observe the oscillations in the experimental hν range. We can roughly examine the eq.(1) for the following cases, (i) $\Theta(r)$ has a non zero value around r= 3.5Å and (ii) it has a non zero value around r= 1.0Å. The former is for the case of a large spherical-shell molecule like C_{60}, while the latter is for a smaller shell which may correspond to usual organic molecules. Since the oscillation derived by eq.(1) is due to the cosine term, $\cos(k_n \times 3.5 + const.)$ and $\cos(k_n \times 1.0 + const.)$ are picked out for the examination. In the experimental k_n range ($3 \sim 6$ Å^{-1}), the cosine term for r= 3.5Å decreases and increases across 0 and an oscillation will be observed in $d\sigma_n^{pw}(\mathbf{k}_n)/d\hat{\mathbf{r}}$. On the other hand, the cosine term for r= 1.0Å is hardly changed due to the longer period of the cosine term, and no oscillation will appear. Therefore, it is concluded that the essential factors for the oscillations are (1) the molecular structure of C_{60} like a spherical shell, and (2) the fairly large radius of the shell.

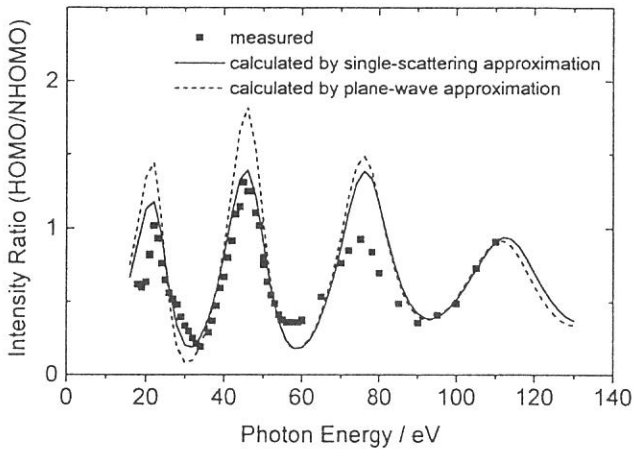

Figure 1 Photon energy hν dependences of photoemission intensity ratio of HOMO/NHOMO. The intensity oscillation of the measured results (solid squares) is in good agreement with the calculated curves. The solid line was calculated by the single-scattering approximation for the final state. The broken line was calculated by the plane-wave approximation for the final state.

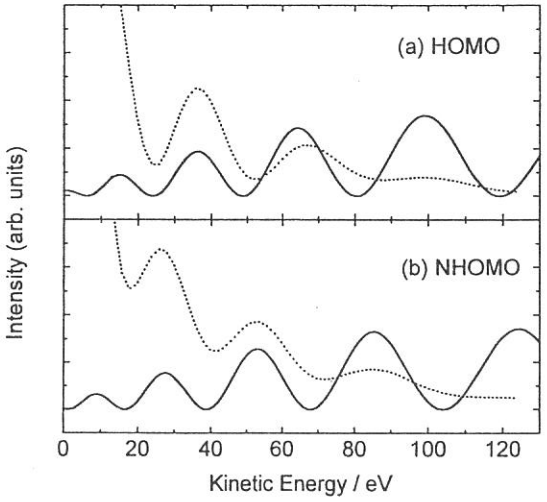

Figure 2 Calculated hν dependences of photoionization cross section. The solid curves were calculated with the spherical-shell like initial state and the plane-wave final state, where R_s= 3.26Å, Δ= 0.5Å and V_0= -10eV.

REFERENCES

[1] P. J. Benning *et al.*, Phys. Rev. B, **44**, 1962 (1991)., J. Wu *et al.*, Physica C, **197**, 251 (1992)., T. Liebsch *et al.*, Phys. Rev. A, **52**, 457 (1995).

[2] Y. B. Xu, M. Q. Tan, and U. Becker, Phys. Rev. Lett., **76**, 3538 (1996).

[3] S. Hasegawa *et al.*, Phys. Rev. B, **58**, 4927 (1998).

(BL8B2)

Angle-resolved UPS of Poly(2-vinylnaphthalene) thin films

K.K.Okudaira, Y.Azumai, K.Meguro, S.Hasegawa[A], K.Seki[B],Y.Harada[C], and N.Ueno[A]

Graduate School of Science and Technology, Chiba University, Chiba 263-8522
[A]*Institute for Molecular Science. Okazaki, 444-8585*
[B]*Faculty of Science, Nagoya University, Nagoya 464-8602*
[C]*Department of Material Science, Faculty of Engineering, Chiba University, Chiba 263-8522*

Thin films of pendant group polymers are the most promising candidates for practical use due to their stability and facility of preparation. Furthermore, their surface properties can be easily controlled by changing the pendant chemical group. However, in general the molecules in polymer solids are not ordered due to the large molecular-weight distribution and mixed tacticy, etc., and therefore it is believed that the pendant groups are also unoriented at the surface.

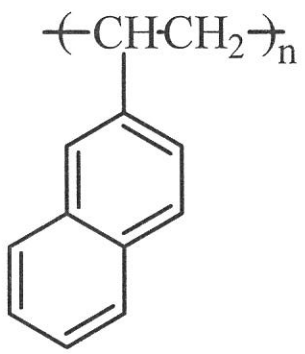

Figure 1 Molecular structure of Poly(2-vinylnaphthalene)

In this work the electronic structure and orientation of pendant groups of poly(2-vinylnaphthalene) (PvNp) (Fig.1) thin films were investigated by angle-resolved ultraviolet photoelectron spectroscopy (ARUPS) using synchrotron radiation. The ARUPS offers information on the geometrical structure of thin films as well as on their electronic structure. For example, we could determine the structure of thin films consisting of large organic molecule such as of 3,4,9,10-perylenetetracarboxylic dianhydride by the analyses of ARUPS intensities.[1] Furthermore we recently found that the orientation of the pendant group of polystyrene at the film surface depends on film thickness.[2]

ARUPS measurements were carried out at the beamline BL8B2 of the UVSOR at the Institute for Molecular Science. ARUPS spectra were measured at hν=40eV and at normal incidence (incidence angle of photon α=0°). Thin films of PvNp were prepared by spincasting on Au-evaporated Si(100) wafers from toluene solutions of 0.3wt/vol%. The film thickness prepared in this way is about 100Å.

Figure 2 shows the ARUPS spectra of the PvNp thin film as a function of the take-off angle (θ). The intensity of top band A shows slight θ dependence. The calculated density-of-states (DOS) using molecular orbital (MO) calculation (STO-6G) is also shown in Fig.2. The MO calculation was performed for a model compound [CH_3-$CH(C_{10}H_7)$-CH_3] of the polymer unit, and the DOS was obtained by a Gaussian broadening (FWHM = 0.8 eV) of the MO levels. The agreement between the observed

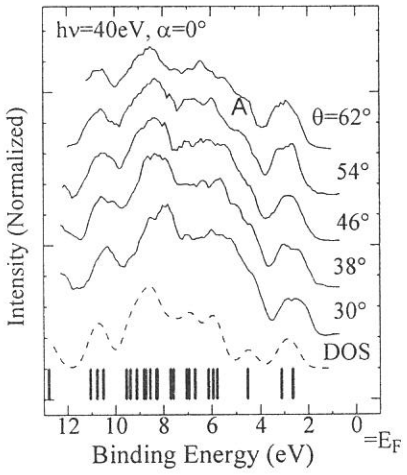

Figure 2 ARUPS of PvNp thin films spincasted from 0.3 wt/vol% toluene solution at hν=40eV and α=0° as a function of take-off angle (θ). The vertical bars show the molecular orbital energies calculated by *ab initio* MO calculation (STO-6G). The density of states (DOS) is represented by (– – – – –) (see text). The calculated binding energy scale was contracted by 1.35 and shifted to fit with the experimental results.

spectra and the DOS indicates that the electronic structure of PvNp is well simulated by that of the model compound. The band A in the spectra originates from two top π states at the pendant naphthalene, and hereafter we focus on the θ dependence of the intensity of the band A to determine the orientation of the pendant naphthalene groups at the surface.

In order to obtain the molecular orientation of the pendant naphthalene, we made the analyses of the θ dependence in the single-scattering approximation combined with molecular orbital (SS/MO) approximation.[3] The calculations were performed for the model compound. The phase shift and radial matrix element were calculated for all subshells of the atoms constituting the molecules using the Muffin-tin potential,[4] and the potential between the Muffin-tin spheres was assumed to be zero. In the present calculation we used the phenomenological electron mean-free path of 8 Å to calculate the damping factor.[3] We further assumed an azimuthal disorder for the rotational orientation of the pendant naphthalene groups with respect to the surface normal. For the calculation of photoelectron intensity, we introduced an inclination angle (β) of the molecular plane of pendant naphthalene groups with respect to the film surface.

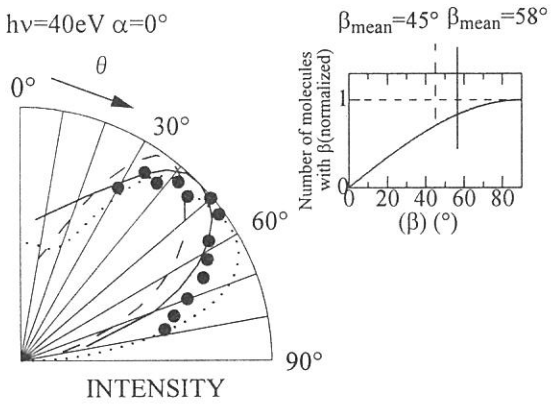

Figure 3 Comparison between calculated and observed (●) take-off angle (θ) dependences of the intensity of the band A. All calculations were carried out by the SS/MO approximation. The calculated result for 3-dimensional isotropic orientation shown in the inset is represented by (———). The calculated result for a uniform distribution shown in the inset is represented by (– – – – –). The calculated result for β=57° is represented by (·····).

In Figure 3 the observed θ dependence of the intensity of the band A is compared with calculated results, for (i) 3-dimensional isotropic orientation which gives a mean value of β (β_{mean}) of 58° shown in the inset of Fig.3, (ii) a uniform distribution of β (β_{mean}=45°), and (iii) a system where all pendant naphthalene groups tilt at 57°. It is seen that the calculated θ pattern for the case (i) gives the best agreement. The β_{mean} of 58° obtained by the analyses of ARUPS is in good agreement with the β of 57° determined by the NEAXFS study.[5] From these results we conclude that the tilt angle of the pendant naphthalene groups at the film surface have a distribution with a mean value of about 58°.

The ARUPS study offers the tilt-angle distribution as well as its mean value

REFERENCES

[1] Y. Azuma, T. Hasebe, T. Miyamae, K. K. Okudaira, Y. Harada, K. Seki, E. Morikawa, V. Saile, and N. Ueno, J. Synchrotron Radiation **5**, 1044 (1998).

[2] N. Ueno, Y. Azuma, M. Tsutsui, K. K. Okudaira, and Y. Harada, Jpn. J. Appl. Phys. **37** 4979 (1998).

[3]N.Ueno, A.Kitamura, K.K.Okudaira, T.Miyamae, S.Hasegawa, H.Ishii, H.Inokuchi, T.Fujikawa, T.Miyazaki, and K.Seki, J.Chem.Phys., **107** 2079(1997).

[4]D.Dill and J.L.Dehmer, J.Chem.Phys., **61** 692 (1974).

[5]K. K. Okudaira, E. Morikawa, D.A.Hite, S. Hasegawa, H. Ishii, M. Imamura, H. Shimada, Y. Azuma, K. Meguro, Y. Harada, V. Saile, K. Seki, and N. Ueno,J.Electron Spectrosc.Relat.Phenom, accepted

(BL8B2)

Electronic structure of poly(1,10-phenanthroline-3,8-diyl) and its K-doped state studied by ultraviolet photoelectron spectroscopy

T. Miyamae [a], Y. Saito [b], T. Yamamoto [b], S. Hasegawa [a], K. Seki [c], and N. Ueno [a,d]

[a] *Institute for Molecular Science, Myodaiji, Okazaki 444-8585*

[b] *Research Laboratory of Resources Utilization, Tokyo Institute of Technology, 4259 Nagatsuta, Midori-ku, Yokohama 226-8503*

[c] *Department of Chemistry, Faculty of Science, Nagoya University, Chikusa-ku, Nagoya 464-8602*

[d] *Department of Materials Science, Faculty of Engineering, Chiba University, Inage-ku, Chiba 263-8522*

Families of π-Conjugated polymers are receiving much attention because of their interesting optical and electronic properties. Also such studies of interaction between metal atoms and conjugated polymers can be regarded as a kind of model system of metal/polymer interface formed at the fabrication of organic electroluminescent devices. Poly(1,10-phenanthroline-3,8-diyl), denoted PPhen hereafter, exhibits n-type conducting properties due to the electron-deficient nature of phenanthroline.[1] Its molecular structure is shown in Fig. 1. In this work, we report UPS studies of PPhen and discuss its electronic states. We also studied the changes in electronic structure upon *in situ* doping with potassium by UPS. In order to obtain deep understanding of the electronic states derived by doping, we simulated the UPS spectra of the model compounds using the single-scattering (SS) approximation combined with MO calculations.

The UPS spectra were measured with an angle-resolving UPS spectrometer at BL8B2 of UVSOR Facility. Thin films of PPhen were prepared on gold coated Si (100) substrates by vacuum. Potassium doping of PPhen was carried out *in situ* using a SAES K-getter source. The MO calculations were carried out with a MOPAC 6 program. The calculations of photoemission intensities with SS approximations were carried out on the IBM SP2 computer at the Computer Center of IMS.

The UPS spectrum of PPhen at $h\nu$ = 40 eV is shown in Fig. 2. From the right-hand onset T, the threshold ionization energy (I_{th}) was found to be 6.0 eV. The value of I_{th} of PPhen indicates that acceptor doping to the polymer should be difficult due to the large I_{th}. This large value of I_{th} is consistent with the fact that PPhen is inert against p-type doping (oxidation).[1]

The UPS spectra of K-doped PPhen for increasing doping levels are shown in Fig. 3. By a slight doping with potassium (Fig. 3, curve b), Fermi energy shifts to the lower binding energy side by 0.57 eV. At the intermediate stage of doping (Fig. 3, curves c and d), two new states BP1 and BP2 appear in the band gap region. With increasing the doping level, these peaks gradually grow up, and the position of the Fermi level is further shifted toward the vacuum level by 0.24 eV.

From the comparison with our previous UPS studies of K-doped PBPy,[2] the two states BP1 and BP2 which appeared by the doping can be assigned to the formation of bipolarons. The gap state at 3.94 eV is assigned to the LUMO stabilized by geometric relaxation and filled by electron donation from K atom, while the 5.94 eV peak is the destabilized HOMO due to the geometry modifications to quinoid structure. In addition, the highest lying state in the undoped polymer, peak A, shows decrease of intensity with increasing K content, as illustrated in the Fig. 4 (a). This is consistent with the picture that the formation of bipolaron states leads to the removal of a state from the valence band edge of the neutral molecule to form new states within the band gap. The intensity of peak B also decreases with increasing K doping, indicating that the lone pairs of N atoms of phenanthroline units interact with the K cations. This suggests that the K dopants are preferentially located close to the N atoms of phenanthroline unit.

Next, we will discuss the changes in observed UPS spectra described above by using the simulated UPS spectra obtained by the combination of the MO calculations and the SS approximations. Since K doping of PPhen forms bipolaron bands and the dopant are probably located close to the N atoms of phenanthroline unit, we performed semiemperical MO calculations of phenanthroline-tetramer and its doped systems assuming simplified model systems. For K-doped PPhen, two K cations are located close to the two neighboring phenanthroline dianion units. Potassium-doped PPhen takes a quinoidal character at the inner two units, and the chain becomes nearly coplanar, the torsion angle changing from 44.2 ° to 0 ° in spite of its steric hindrance. We find from the total charge per unit that most of the charges donated from K is transferred to the inner units, only 6 % going to the outer units. The geometry of the outer units is almost the same as that in the undoped case. These results indicate that the charges transferred to the next nearest-neighbor units should be fairly small. After the MO levels of each model compound were obtained from MO calculation, the photoelectron spectra were calculated with the SS approximations. In this method, a random molecular orientation was assumed. In Figs. 4 (a) and 4 (b), we show the measured and calculated UPS difference spectra between K-doped and pristine PPhen in the most intriguing energy region from the vacuum level to binding energy E_b = 14 eV. A good correspondence is obtained between the measured and calculated results, well reproducing the observed positive

peaks located at 4.96 eV and 6.65 eV, due to the formation of bipolaron bands, and the negative peak located at 8.02 eV due to the removal of the states from the valence band edge. The good agreement between the difference spectra confirms that the bipolaron states are generated by the K doping. The relative intensity of BP1 and BP2 is different between the observed and calculated spectra. The observed intensity of BP1 is about one third of the observed intensity of BP2. This disagreement can be reasonably ascribed to a smaller dopant concentration in the observed spectrum than in the calculated one, which corresponds to 50 % doping level.

REFERENCES

[1] Y. Saitoh and T. Yamamoto, Chem. Lett. 785 (1995).

[2] T. Miyamae, D. Yoshimura, H. Ishii, Y. Ouchi, K. Seki, T. Miyazaki, T. Koike, and T. Yamamoto, J. Chem. Phys. **103**, 2738 (1995).

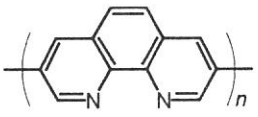

Figure 1. The molecular structure of poly(1,10-phenanthroline-3,8-diyl) (PPhen).

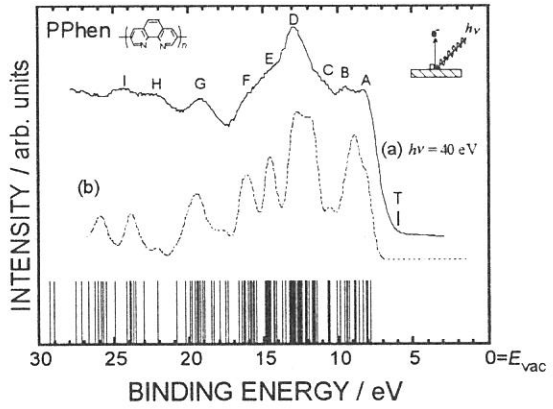

Figure 2. (a) UPS spectra of PPhen using synchrotron radiation of 40 eV. (b) The density of states derived MO calculation of phenanthroline tetramer. The vacuum level (E_{vac}) is taken as the origin of the energy scale. The vertical bars indicate the orbital energies. T denotes the threshold ionization energy.

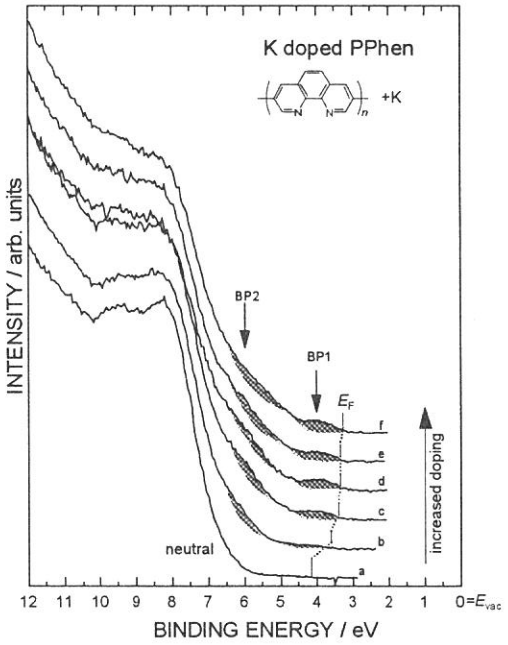

Figure 3. UPS spectra of neutral and increasingly potassium-doped PPhen.

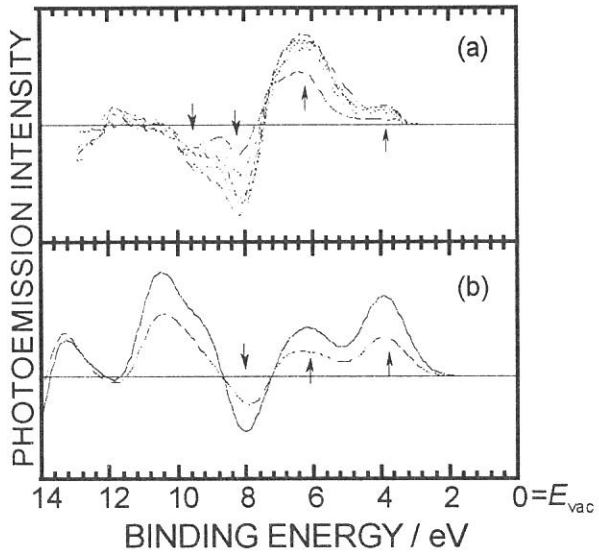

Figure 4. (a) Corresponding difference UPS spectra (UPS_{doped} – $UPS_{pristine}$) obtained by subtracting the spectrum of pristine PPhen from those of K-doped states and (b) corresponding difference UPS spectrum (UPS_{doped} – $UPS_{pristine}$) calculated for tetramer.

(BL8B2)

Ultraviolet Photoelectron Spectroscopy of Poly(anthraquinone)s; Their Electronic Structure and K-Doped States

T. Miyamae[a], T. Yamamoto[b], Y. Sakurai[c], K. Seki[c], and N. Ueno[a,d]

[a] *Institute for Molecular Science, Myodaiji, Okazaki 444-8585*
[b] *Research Laboratory of Resources Utilization, Tokyo Institute of Technology, 4259 Nagatsuta, Midori-ku, Yokohama 226-8503*
[c] *Department of Chemistry, Faculty of Science, Nagoya University, Chikusa-ku, Nagoya 464-8602*
[d] *Department of Materials Science, Faculty of Engineering, Chiba University, Inage-ku, Chiba 263-8522*

π-Conjugated polymers have been the subjects of steadily growing interest in the past 20 years because of their unique and interesting structural and electronic properties. Recently we have found that poly(2methylanthraquinone-1,4-diyl (P(2Me-1,4-AQ), Fig. 1(a)) and poly(anthraquinone-1,5-diyl) (P(1,5-AQ), Fig. 1(b)) exhibit n-type conducting properties.[1)] In this work, we report experimental and theoretical studies of polyanthraquinones (PAQ)s, and discuss their electronic structures. We also studied the changes in electronic structure of PAQs upon doping with potassium by UPS

The P(2Me-1,4-AQ) and P(1,5-AQ) films were prepared by spin-coating from a solution of the polymer in CH_3Cl. The UPS spectra were measured by an angle-resolving UPS spectrometer at BL8B2. Potassium doping of PAQs was carried out *in situ* at 125 °C ± 5 °C using a SAES K-getter source.

The UPS spectra of P(2Me-1,4-AQ) obtained by synchrotron radiation of $h\nu = 40$ eV are shown in Fig. 2 (a). For comparison, in Fig 2 we also show the orbital energies obtained from the PM3 semiempirical calculations of anthraquinone-dimer by vertical lines, and the simulated spectra as the density of states (DOS). According to the calculation, the peak A is formed by the overlapping π and n bands derived from the uppermost-occupied orbitals of anthraquinone, where n denotes the lone pair orbitals of the O atoms. From the right-hand onset T, the threshold ionization energy (I_{th}), was found to be 6.4 eV. The value of I_{th} of P(2Me-1,4-AQ) indicates that acceptor doping of the polymers should be difficult due to the large I_{th}.

In Fig. 3, we show a series of UPS spectra of P(2Me-1,4-AQ) taken at different doping levels with potassium, at the steps from the pristine state to the heavily doping level. At the intermediate stage of doping (Figs. 3 c, d, e), only one new state appears in the energy gap region. Furthermore, no significant change of the work function (-0.24 eV) was observed at the whole doping region. In general, n-type doping of a conjugated polymer results in a decrease in the work function, i.e. a shift in the Fermi energy to lower binding energy, corresponding to the creation of new occupied states in the original energy gap region. The reason for the appearance of only one state and the absence of the change in the work function in K-doped P(2Me-1,4-AQ) may be that the polymer chain cannot take electrons from the dopants effectively to create the bipolarons. According to the electrochemical reduction of 2-methylanthraquinone, radical anion and dianion of anthraquinone are formed.[1)] In the case of P(2Me-1,4-AQ), the electron donation from potassium may lead to the formation of the reduced radical anion and dianion units. From the MO calculation of K-anthraquinone-dimer, each carbonyl group accepts c.a. –0.37 e extra charge at the doped state as compared to pristine polymer. This result indicates that the extra charges are localized at each carbonyl group of anthraquinone unit as radical anion or dianion. Thus we consider that K-doped P(2Me-1,4-AQ) contains the neutral, radical anion, and dianion units.

In contrast to the case of P(2Me-1,4-AQ), P(1,5-AQ) showed poor reactivity to the dopant (not shown). The difference between K-doped P(2Me-1,4-AQ) and K-doped P(1,5-AQ) may be caused by their conformational differences of polymer chain. Optimized geometries of these polymers, which are carried out with a molecular mechanics calculation, were illustrated in the inset of Fig. 3. From the molecular mechanics calculation, the polymer chain of P(2Me-1,4-AQ) has analogous structure with poly(*p*-phenylene), and its anthraquinone units protrude from the main chain, as shown in the inset of Fig. 3. In contrast to the case of P(2Me-1,4-AQ), the polymer chain of P(1,5-AQ) has rather helical structure. Thus we can summarize the P(1,5-AQ) show only a weak ability to coordinate with potassium presumably because of its helical geometry.

1. T. Yamamoto and H. Etori, *Macromolecules*, **28**, 3371 (1995).

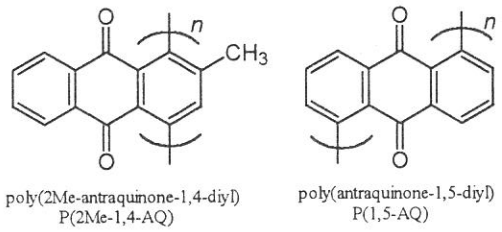

Figure 1 The molecular structure of P(2Me-1,4-AQ) (a) and P(1,5-AQ) (b),

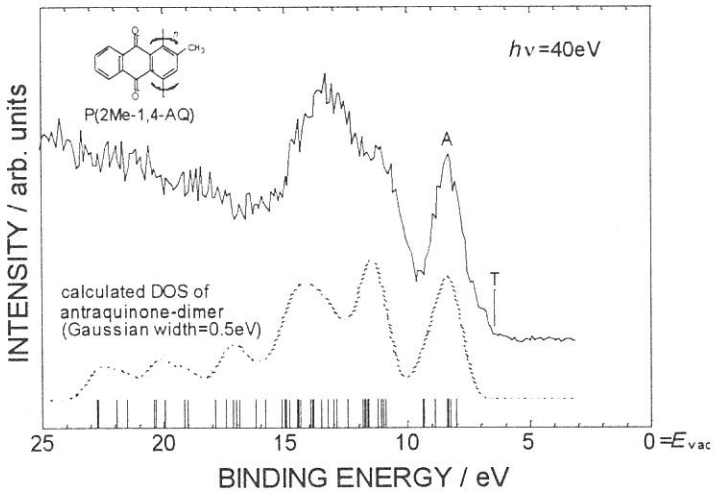

Figure 2 Observed (solid line) and simulated (dotted line) UPS spectra of P(2Me-1,4-AQ) film (a) and PPhen film (b). The vertical lines show the calculated orbital energies. T denotes the threshold ionization energy.

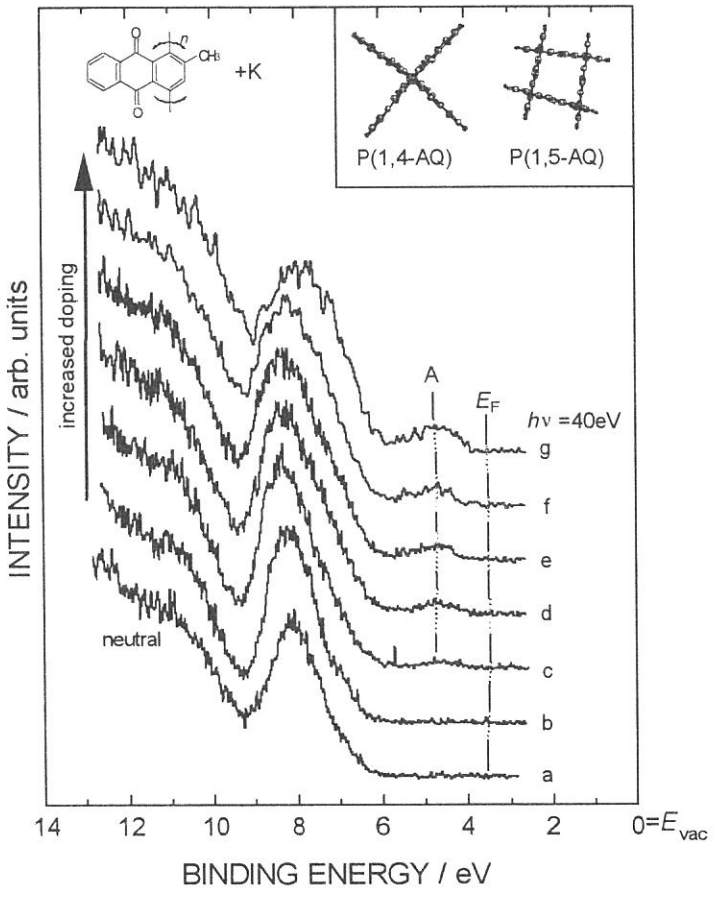

Figure 3 UPS spectra of neutral and increasingly potassium-doped P(2Me-1,4-AQ). The inset shows the projection along the chain axis for P(1,4-AQ) and P(1,5-AQ).

(BL8B2)

Electronic structure of Alq_3/insulator/Al interfaces studied by ultraviolet photoelectron spectroscopy.

T. Yokoyama[a], D. Yoshimura[a], E. Ito[b], S. Hasegawa[c], H. Ishii[a], and K. Seki[d],

a) Department of Chemistry, Faculity of science, Nagoya university, Nagoya 464-8602

b) Venture business laboratory, Nagoya university, Nagoya 464-8603

c) Institute of Molecular science, Myodaiji, Okazaki 444-8585

d) Research center of material science, Nagoya university, Nagoya 464-8602

Recently, organic electroluminescent (EL) devices have attracted much attention in close relation to the application to display technology. The interfacial electronic structure of such devices, which dominates the carrier injecting properties, is key issue for understanding and improvement of the performance of the devices. Very recently, the improvement of the device performance by the insertion of very thin insulating layer such as PMMA, LiF and aluminum oxide between a cathode electrode and electron-transporting layer (ETL) has been reported by several groups. In spite of the extensive studies, the mechanism of the improvement has not been well understood. The elucidation of the electronic structures of the cathode/ insulator and the insulator/ETL interfaces is indispensable for clarifying the mechanism.

In this work we investigated the electronic structure of tris(8-hydroxyquinolino)alminum (Alq3 (Fig1))/insulator (LiF and Aluminum oxide)/Al systems using ultra violet photoelectron spectroscopy (UPS) system at BL8B2 of institute of molecular science. The film thickness of Alq3 and LiF was measured with crystal oscillator. Aluminum oxide film was prepared by exposing the clean Al surface to the air for an hour.

Figs. 2(a)-(c) show the energy diagrams of Alq3/Al, Alq3/LiF/Al, and Alq3/Al oxide/Al interfaces obtained from the UPS results. In the case of Alq3/Al, the shifts of vacuum level(Δ) of -1.0 was observed. Because of this downward shift, lowest unoccupied molecular orbital (LUMO) is close to the Fermi level of the Al electrode, inducing the small barrier height for electron injection as shown in Fig.2(a). In the case of Alq3/LiF/Al, the vacuum level shifts of −1.0 and −0.2 eV were observed at Al/LiF and LiF/Alq3 interfaces, respectively. The total vacuum level shift between Al and Alq3 was −1.2 eV and were larger than that at Alq3/Al interface, suggesting the decrease of the barrier height for electron injection by LiF layer. Such decrease of the barrier height for electron injection is probably one of the possible origins of the improvement effect by insulating layer.

At Alq3/Al oxide/Al interfaces, the vacuum level shift of −1.0eV was observed at Al oxide/Al interface as in the case of LiF/Al and Alq3/Al interfaces, while no significant shift was observed at Al oxide/Alq3 interfaces. The total shift of −1.0 eV was similar to that at Alq3/Al interface. Thus we cannot expect the improvement of the device performance. This discrepancy can lead two possible explanations: first is that the other origin for the improvement effect rather than the

decrease of the barrier height should be considered. Second is that the difference of the surface preparation between our experiment and the real device can change the barrier height. In order to clarify this point, the UPS measurement of the interface prepared in the real device condition should be performed.

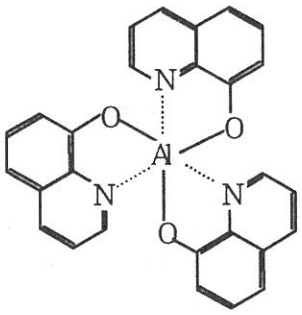

Fig1 Chemical structure of
tris(8-hydroxyquinolino)alminum (Alq3)

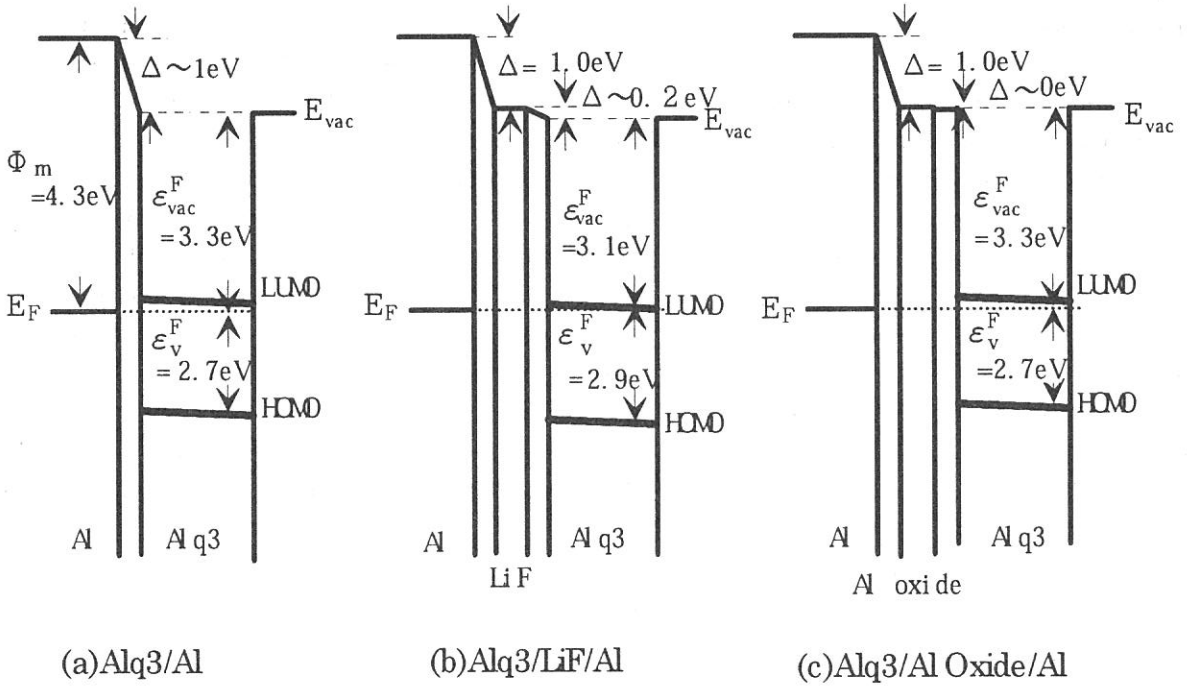

(a)Alq3/Al (b)Alq3/LiF/Al (c)Alq3/Al Oxide/Al

Fig2 Energy diagram of Alq3/insulator/Al interfaces

(BL8B2)

UV Photoelectron Spectroscopy of Polycarbosilane

Y. Sakurai[a)], D. Yoshimura[a)], H. Ishii[a)], H. Isaka[b)], H. Teramae[b)],
N. Matsumoto[b)], S. Hasegawa[c)], N. Ueno[c)], and K. Seki[d)]
a) Department of Chemistry, Faculty of Science, Nagoya University, Nagoya 464-8602
b) NTT Basic Research Laboratories, Morinosato-Wakamiya, Atsugi, Kanagawa 243-0198
c) Iistitute for Molecular Science, Myodaiji, Okazaki 444-8585
d) Reserch Center of Material Science, Nagoya University, Nagoya 464-8602

Polysilane and polyethylene have homocatenated skeletons composed of silicon and carbon atoms, respectively. Polysilanes, whose electronic structure is characterized by σ-conjugation along the Si backbone, have attracted much attention as a new class of photoresists, conducting polymers, and emitting materials in organic light-emitting diode. While polyethylenes have also σ-conjugation along the C backbone, the σ-conjugation does not dominate the electronic properties of polyethylenes, because the ionization potentials of the σ-conjugated
orbitals are quite larger. Electronic structure of polycarbosilane whose backbone consists of silicon and carbon is expected to differ from those of the homopolymers. In this work, by using ultraviolet photoelectron spectroscopy (UPS), we investigated the electronic structure of polycarbosilane which consists of repeating Si_2C units, and compared the observed electronic structure with those of polysilane and polyethylene.
The sample was synthesized at NTT. The samples used in the UPS measurements were prepared on a copper disk by spin coating of 0.2wt% toluene solution. UPS spectra were measured using angle-resolved UPS system at BL8B2 of UVSOR at Institute for Molecular Science. Ionization threshold energy was measured by the photoelectron spectrometer with a retarding field analyzer and a helium discharge lamp (hν = 21.2 eV) in Nagoya university.

The UPS spectrum of polycarbosilane $[(SiMe_2)_2CH_2]_n$ at hν=40eV is shown in Fig. 1(a). The abscissa is the binding energy relative to the vaccum level. The spectrum has four structures labelled by A, B, C and D. For comparsion, reported gas-phase UPS spectra of Si_2Me_6 and Si_4Me_{10}[1)] with the peak assignments are shown in Fig. 1(b) and (c). The energy axes of gas-phase spectra were adjusted to align the SiC peaks with peak B in the UPS spectrum of polycarbosilane. From the comparsion among the spectra, we assigned feature A to Si-Si bond, feature B to Si-C bonds, feature C to C-H bonds, and feature D to C_{2s}. The peak due to Si-Si bond extends to lower binding-energy side than those of Si_2Me_6, and the lineshape is similar to that of Si_4Me_{10} in shape. This suggests that each Si-Si units, which are separeted by a carbon atom, still interact with each other, forming σ-conjugation of the backbone.
In Fig. 2 (a) - (c), UPS spectrum of polycarbosilane and the density of states (DOS) obtained from 3-21G *ab-initio* and PM3 MOPAC calculations. The calculated results agree well with the UPS spectrum. The analysis of the molecular orbital patterns demonstrated that the molecular orbitals due to the Si-Si bond are actually delocalized over the molecule. Such σ-conjugation is also supported by the observed ionization potential. The observed ionization potential of polycarbosilane was 6.4 eV. This value is between those of polysilanes (5.9eV)[2)] and polyethylene (8.5eV)[3)], indicating that the degree of σ-conjugation of polycarbosilane is smaller than those of polysilanes.

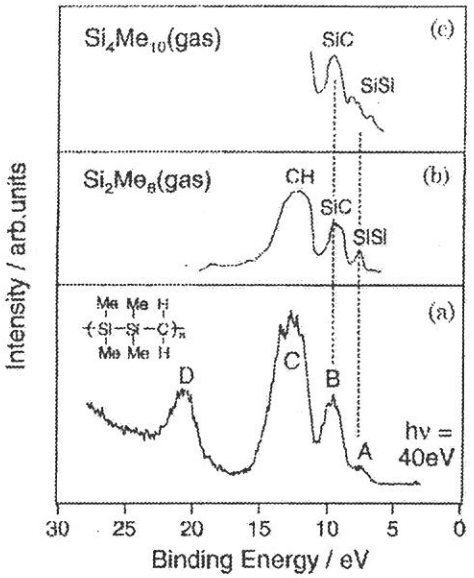

Figure 1. (a)UPS spectrum of polycarbosilane at hν = 40 eV, (b)UPS spectrum of gas-phase Si_2Me_6, (c)UPS spectrum of gas-phase Si_4Me_{10}.

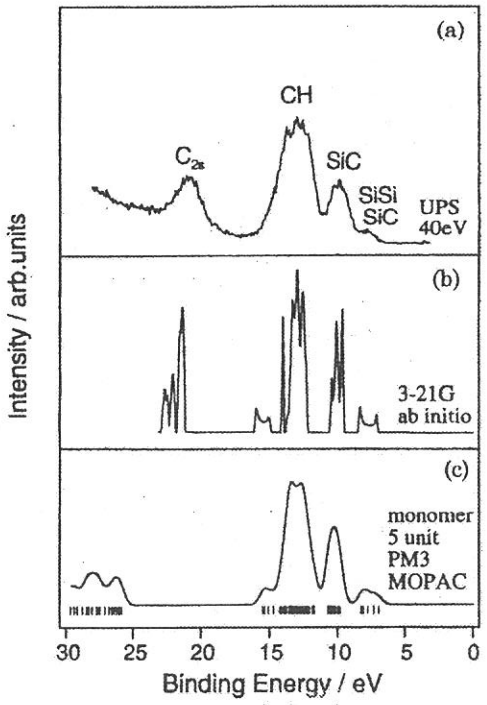

Figure 2. (a)UPS spectrum of polycarbosilane at hν = 40 eV, (b)the calculated density of states by 3-21G ab initio molecular orbital calculation, (c)the calculated density of states by PM3 MOPAC calculation.

References

1) H. Bock and W. Ensslin, Angew. Chem., Int. Ed. Engl., 10,404 (1971)
2) K. Seki, T. Mori, H. Inokuchi and K. Murano, Bull. Chem. Soc. Jpn., 61,351 (1988)
3) M. Fujihira and H. Inokuchi, Chem. Phys. Lett., 17, 554 (1972)